Magnetorheological finishing for removing surface and subsurface defects of fused silica optics Magnetorheological finishing for removing surface and subsurface defects of fused silica optics

Jérôme Neauport, Rodolphe Catrin, Daniel Taroux, Philippe Cormont, Cédric Maunier, Sébastien Lambert

Optical Engineering

SPIEDigitalLibrary.org/oe

Magnetorheological finishing for removing surface and subsurface defects of fused silica optics

Rodolphe Catrin
Jerome Neauport
Daniel Taroux
Philippe Cormont
Cedric Maunier
Sebastien Lambert

Magnetorheological finishing for removing surface and subsurface defects of fused silica optics

Rodolphe Catrin,[a] Jerome Neauport,[a,*] Daniel Taroux,[a] Philippe Cormont,[a] Cedric Maunier,[a] and Sebastien Lambert[b]
[a]Centre d'Etudes Scientifiques et Techniques d'Aquitaine, Commissariat à l'Energie Atomique et aux Energies Alternatives, CS60001, F-33116 Le Barp, France
[b]Centre du Ripault, Commissariat à l'Energie Atomique et aux Energies Alternatives, F-37260 Monts, France

Abstract. We investigate the capacity of magnetorheological finishing (MRF) process to remove surface and subsurface defects of fused silica optics. Polished samples with engineered surface and subsurface defects were manufactured and characterized. Uniform material removals were performed with a QED Q22-XE machine using different MRF process parameters in order to remove these defects. We provide evidence that whatever the MRF process parameters are, MRF is able to remove surface and subsurface defects. Moreover, we show that MRF induces a pollution of the glass interface similar to conventional polishing processes. [DOI: 10.1117/1.OE.53.9.092010]

Keywords: magnetorheological finishing; polishing; laser damage; fused silica.

Paper 140284SS received Feb. 18, 2014; revised manuscript received Apr. 24, 2014; accepted for publication Apr. 30, 2014; published online May 22, 2014.

1 Introduction

Magnetorheological finishing (MRF) technology is commonly used in optical workshops to finish optical surfaces. The use of MR fluids for precision finishing of optical components was proposed in the early 1990s based on Belarus studies of physical properties of these fluids.[1] It was further developed in the 1990s in the United States[2,3] to become a commercial product.[4] MRF uses magnetic carbonyl iron and nonmagnetic abrasive particles (diamond, cerium) mixed in water and some additives as polishing fluid. Since iron particles are magnetic, the rheology of the fluid can be modified by the application of a magnetic field. This MR polishing slurry is circulating on a delivery system and put in contact with the workpiece due to a polishing wheel in the vicinity of which the field is applied. Material removal is the result of both drag force and normal force induced by the MR ribbon stiffened by the magnetic field.[5] The good stability of material removal along the process allows iterative subaperture polishing. MRF is used for a wide variety of applications, such as plane, spherical, aspherical, or freeform surface polishing[6–8] and phase plate manufacturing, as well as high-damage-threshold laser fusion fused silica optics polishing.[9,10] MRF is usually used as a final polishing step that follows grinding and prepolishing.

Cosmetic surface quality is most of the time detrimental for optical components. Scratches, digs, voids, or other residual chips on the surface can stray light, degrade optical system performances, or degrade damage threshold in the case of laser optics. Such defects can be created by inappropriate handling or cleaning, rogue particles existing in polishing slurry acting as indents on the glass surface or also insufficient material removal leaving traces of subsurface fractures coming from early manufacturing steps. Consequently, the ability of a polishing process to limit or suppress surface defects is important. Polishing fused silica optics able to withstand high fluence at the wavelength of 351 nm is even more demanding. Subsurface defects (SSD)[11,12] as well as surface defects and potential process-induced contamination[13–15] are likely to trigger laser damage and thus need to be removed from the polished interface. It must be outlined that for polished surfaces, the interface is composed of (i) subsurface cracks coming from either early manufacturing steps (grinding, lapping, etc.) or final polishing and embedded under a polishing layer and (ii) open cracks appearing as scratches or digs and coming from either rogue polishing particles during polishing or residual cracks from previous manufacturing steps.

The goal of this report is to focus on the capabilities of MRF to remove surface and subsurface defects in the context of the manufacturing of fused silica laser fusion optics. Characterizations are also carried out to quantify the MRF-induced pollution of the interface. Although previous works on MRF have detailed numerous potential application of MRF, physical phenomena inducing material removal,[5,16–18] influence of process parameters on material removal,[19] or use of MRF for manufacturing damage resistant optics,[9,10] no systematic study of surface–subsurface defect removal by MRF and MRF-induced interface contamination has been carried out to the best of our knowledge. We report the work as follows. Section 2 describes the sample preparation methods. This includes the initial polishing and the intentional scratching method. In order to increase the statistic of our experiment, we created deliberately random scratches on the samples. The metrology used to characterize these samples is also detailed. Section 2 summarizes the experimental data. In Sec. 3, we discuss how MRF is efficient to remove surface and subsurface defects. Section 4 is more specific to laser damage by giving some details on the polishing layer created by

*Address all correspondence to: Jerome Neauport, E-mail: jerome.neauport@projet-lmj.org

0091-3286/2014/$25.00 © 2014 SPIE

MRF, its composition and thickness, and also some damage threshold considerations. We then present our conclusions.

2 Experimental Results

2.1 *Fused Silica Samples Polishing and Scratching Process*

Fused silica was studied in this work. This optical glass is usually used as substrate for the final optics of fusion class lasers for its low absorption, high homogeneity, and high damage threshold at the wavelength of 351 nm.

All substrates were disks with a diameter of 50 mm and a thickness of 8 mm, made of CORNING 7980. Samples were polished using a commercially available standard double side polishing process. Surface roughness Ra was less than 1 nm, and scratches and digs comply with a 60/40 specification per MIL-O-13830A standard.

Our intention was to study the efficiency of MRF to remove surface and subsurface defects of polished surfaces. Even if surface and subsurface defects exist on our polished samples, their density is rather weak. The statistic is then too small for such a study to be carried out. We therefore created additional defects by deliberately scratching the samples on one side. This was performed by polishing samples on a LOGITECH PM5 machine using cerium slurry polluted with 0.1 g/l of 9-μm-diameter alumina particles. This procedure was fully detailed in a previous work;[20] it creates a large number of surface and subsurface defects with a scratch morphology similar to what is seen on polished surfaces (see Fig. 1).

2.2 *Magnetorheological Finishing*

MRF was performed using a Q22-XE polishing platform from QED.[4] The C10+ cerium-based slurry distributed by QED was used for our experiments; it was prepared following the manufacturer's recommendations. Samples before and during polishing cycles as well as MRF spots were measured using a Zygo GPI XP 100-mm aperture phase He-Ne Fizeau shifting interferometer. Spots' physical properties (depth, volume, area, etc.) and volumetric removal rates

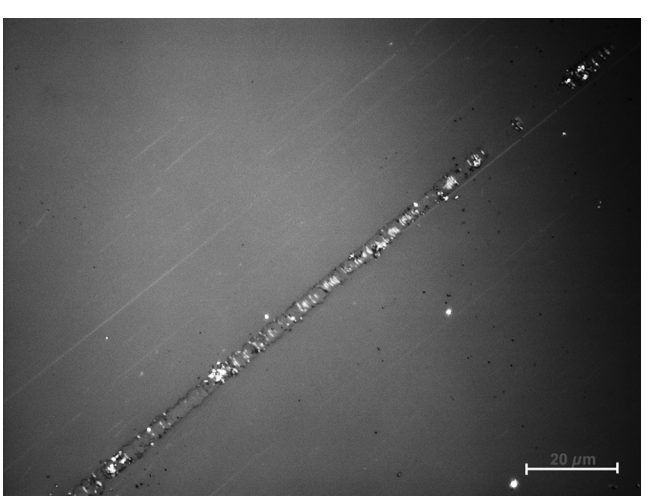

Fig. 1 Scratch created by polishing a sample with a cerium slurry contaminated with 9-μm-diameter particles of alumina (0.1 g/l).

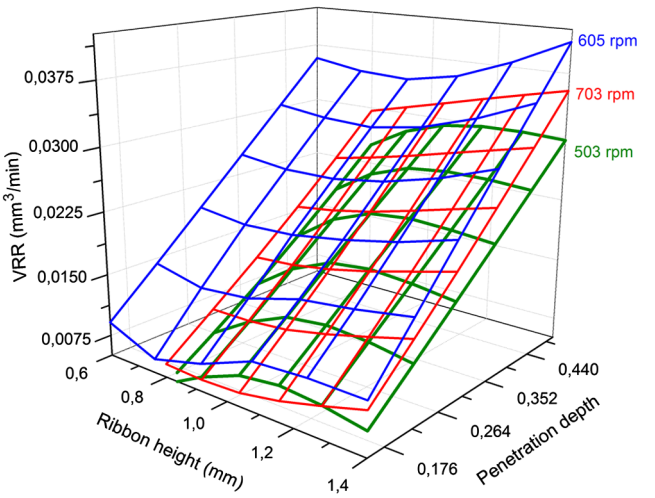

Fig. 2 Effect of magnetorheological finishing (MRF) process parameters on VRR—CORNING 7980 fused silica sample.

(VRR) were calculated from these measurements directly by the Q22-XE software.

Removal rate of the MRF process can be modified by changing wheel speed, penetration depth in the MR ribbon, or ribbon height (magnetic field is fixed on the Q22-XE). The effect of the variation of these parameters on the VRR is shown in Fig. 2. VRR can be modified by almost a factor of four by changing the MRF parameters. For these VRRs, a mean MRF processing time of approximately 30 min is necessary to remove a thickness of 500 nm on a 50-mm-diameter sample.

2.3 *Optical Characterization*

A defect mapping system (DMS) was used to quantify defects existing on polished surfaces before or after MRF processing. This system consists of a lighting LED ring placed around the sample to be measured and a high-resolution 39-Mpx camera equipped with a 120-mm focal lens to take an image of the whole sample clear aperture. Surface defects scatter light coming from the LED ring, thus appearing bright on a dark field.[21] Raw images are then postprocessed using ImageJ[22] software to evaluate the defects' density as bright pixels per square centimeter. A full description of the postprocessing carried out is available elsewhere.[20] The resolution of the system is approximately 30 μm.

A Zygo New View 7200 white light interferometer (WLI) equipped with 1×, 10×, or 100× objectives was used for roughness measurements or local defect or laser damage imaging. Alternatively, we also took advantage of a Zeiss AxioImager microscope equipped with 10×, 20×, 50×, and 100× objectives for immediate imaging of scratches during polishing.

2.4 *Polishing-Induced Contamination Measurement*

During polishing, a layer is formed by the chemo-mechanical action of abrasives and water on the silica glass. This layer, called Beilby layer[23] or polishing layer, can partially embed subsurface defects; it is also contaminated by polishing agents. Beilby layer thickness is usually estimated between

50 and 100 nm for conventional processes. Polishing-induced contamination can also diffuse in the SSD, which can extend far below the polishing layer. We measured this global process-induced contamination by inductively coupled plasma atomic emission spectrometry (ICP-AES). The method consists in dissolving a layer of a silica-polished sample whose thickness is known in a HF/HNO_3 (80% to 20% vol.) solution. This solution is then analyzed by ICP-AES to give access to the quantity of each pollutant included in this known layer. This sequence is then repeated until the concentration of tracked elements reach an asymptote. A full description of this method is available elsewhere.[14] This technique offers the interest of being very sensitive; the quantification limit is close to the ppm and incertitude of about 0.1 ppm depending on the element considered and depth of the silica layer dissolved. Another advantage is that this analysis is carried out on the whole 50-mm-diameter sample surface, in opposition to secondary ion mass spectroscopy methods where a few hundreds of square micrometers are measured. In this study, we measured the following elements: Fe, Ce due to (i) their presence in the manufacturing process (slurry, tools, etc.), (ii) their possible absorption at the wavelength of 351 nm, and (iii) their potential impact on laser damage.[13] Quantification limit for these elements, considering the experimental protocol used, is approximately 1 to 10 $\mu g/g$. If we made the assumption that pollution is mainly trapped in surface and subsurface defects of the glass interface, it implies that ICP method is one or two orders of magnitude more sensitive than the DMS measurement. Strict depth comparison between DMS and ICP shall not be made.

2.5 *Laser Damage Testing*

We carried out damage testing using a 1:1 procedure with respect to ISO 11254-1:2000 standard using a Nd:YAG laser manufactured by Coherent (Santa Clara). The source is frequency tripled with the following characteristics: wavelength of 355 nm and single longitudinal mode and pulse duration of 2.5 ns. During the test, the beam is focused on the sample surface in order to achieve high fluences; beam diameter is then about 400 μm at 1/e. The depth of focus is about 30 cm, much larger than usual sample thickness. Fluence fluctuations have a standard deviation of about 15% for this laser at 355 nm. Spatial and temporal profiles and energy are recorded during test. Damage is observed after laser irradiation using a long-distance working microscope. Minimum damage size detected is about 10 μm whatever the morphology of the damage. The threshold is defined as the zero damage probability.

3 Surface and Subsurface Defects Removal

First, the effect of MRF removal on surface and subsurface was studied on a microscopic scale by following the evolution of the morphology of some scratches. A sample was scratched as described in Sec. 2.1. The DMS image of the scratched sample (S/N 12-0192) is shown in Fig. 3.

An example of scratch morphology during iterative MRF removals is given in Fig. 4. The width of the original scratch was approximately 10 μm (before MRF). Each image of Fig. 4 has been taken after a 500-nm MRF removal. Images were obtained using a Zeiss Axio-Imager microscope in dark interference contrast mode equipped with a 20× objective. Image size is $230 \times 250\ \mu m^2$. After a total 2.5-μm material removal by MRF, the scratch is mostly removed from the surface. This is in good concordance with the relation evidenced by Suratwala et al.[24] estimating mean crack depth to be equal to the third of its width. Directional sleeks are also systematically observed in the vicinity of the pre-existing scratch. Sleeks are oriented along the direction of the MR fluid flow. This phenomenon was already observed and is due to the perturbation of MR ribbon created by the scratch during polishing.[9]

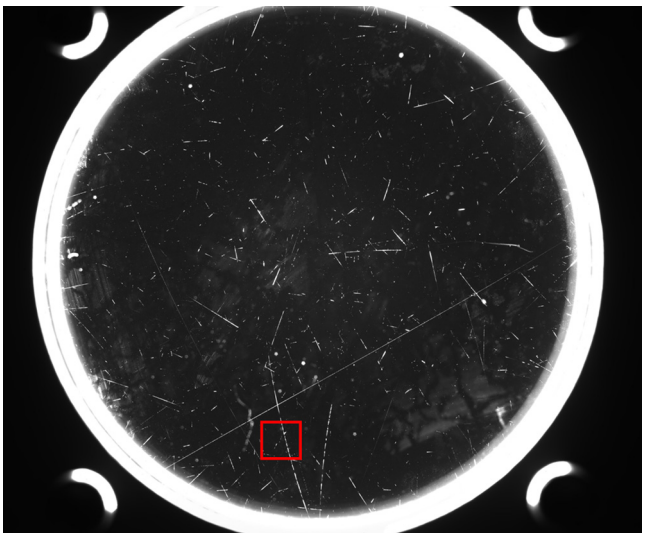

Fig. 3 Sample 12-0192 after scratching procedure. Red square shows the position of the scratch imaged during 500-nm iterative MRF removals.

Second, the effect of MRF on surface and subsurface defects was studied on a large number of scratches. For this purpose, samples were polished and scratched using the protocol described in Sec. 2.1. Initial measurements carried by DMS on a polished and a scratched sample revealed that scratching process increase defect density by more than a decade.

We then iterated numerous sequences of

- cleaning
- DMS for defect counting
- MRF uniform removal
- cleaning
- DMS for defect counting.

Mean VRR during iterative removals was modified by about 25% in order to see its effect on defect removal (see Fig. 5). This corresponds approximately to the mean VRR capacity and maximal VRR capacity of the machine (see Fig. 2). Lower VRRs were not studied since processing times become too long given the high amount of material we wanted to remove (up to 24 μm). DMS images were analyzed using the procedure detailed in Sec. 2.3. Figure 5 represents the evolution of the defect density during these removals. Power law fittings are shown as guidelines.

A decrease of about a decade in defect density is observed after removal of approximately 6 μm. Suratwala et al. established a relationship between width (W) and mean crack depth (d) of cracks existing on the glass polished surfaces:[24]

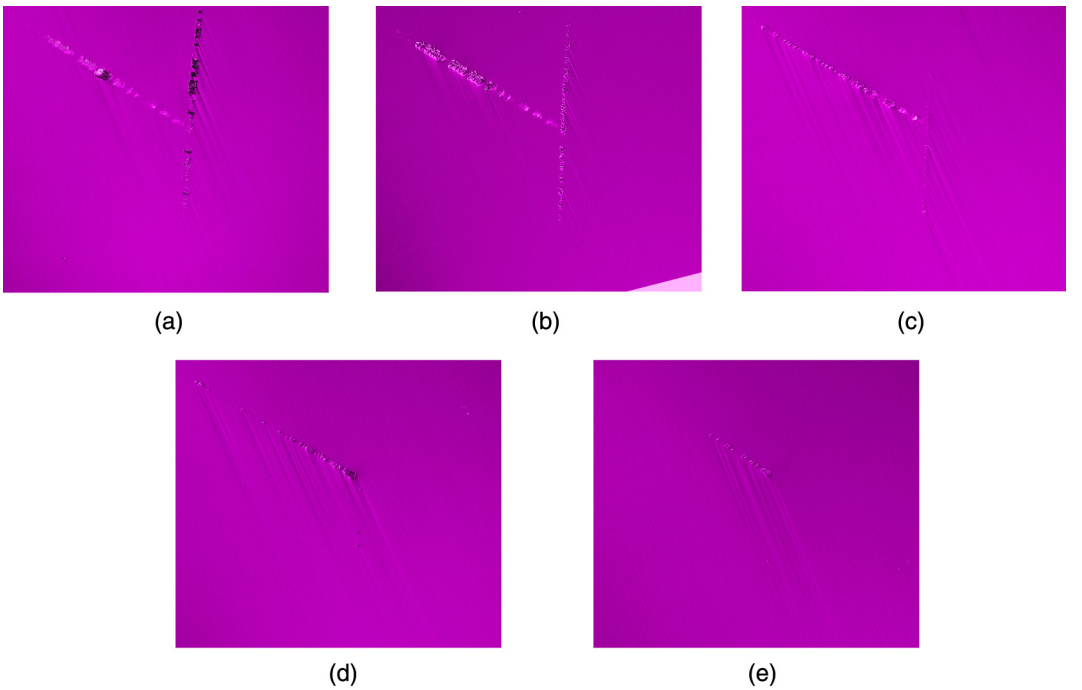

Fig. 4 Evolution of the scratch identified in Fig. 3 after 500-nm MRF removal (a), 1000-nm MRF removal (b), 1500-nm MRF removal (c), 2000-nm MRF removal (d), and 2500-nm MRF removal (e). Image size is 230 × 250 μm.

$d = 0.35W$. This group also evidenced a 90% probability to remove a crack by removing a layer of material equal to the crack width.[25] In our experiment, mean crack width of the scratches generated by the initial scratching procedure (see Sec. 2.1) is 10 μm. After a removal of 3 μm, scratch density decreases by more than half a decade. After approximately 10 μm, a one-decade decrease is seen on sample 12-0192, which is consistent with the 90% probability of scratch removal. On the other samples, data are too widespread to verify this relationship.

We also noticed that DMS measurements become very difficult when defect density is close to some hundreds per centimeter square. The reproducibility of the cleaning process in terms of quality and the ability of the raw image postprocessing to distinguish remaining stains from surface defects become influential. Nevertheless, we also evidence that VRR does not seem to have a large impact on the efficiency of MRF to remove defects. Even for high VRR corresponding to larger penetration depth, where both drag and normal forces are important as evidenced by Miao,[18] cracks are removed and not propagated by the MRF process.

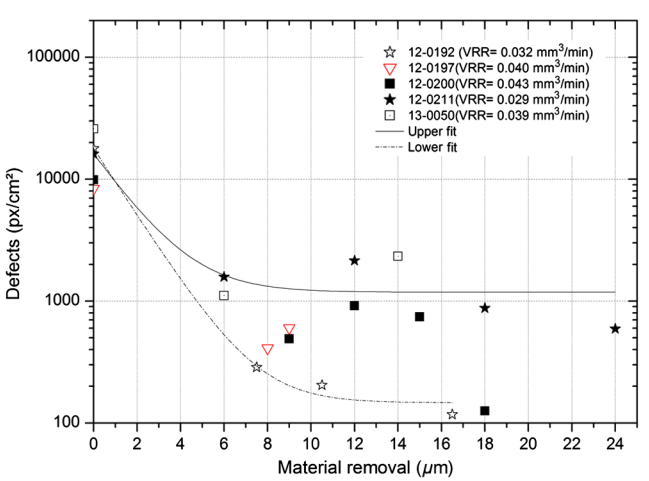

Fig. 5 Evolution of defect density established from defect mapping system measurements during iterative MRF removals with different mean volumetric removal rates. Power fits are represented a guide to the eye.

Moreover, it must be outlined that apart from sleeks surrounding pre-existing scratches (see Fig. 4), close inspection to successive DMS images revealed no MRF-related surface defects.

We performed roughness measurements on some of these samples using apparatus detailed in Sec. 2.3. Roughness was measured on the $[0.1\,\text{to}\,1]_{\text{mm}}$ spectral band using the 1× objective. After 3 μm of uniform removal, a roughness of 0.49 nm RMS was obtained. The value rose to 1.14 nm RMS after 12 μm of removal, which is similar to the 1-nm-RMS initial value of our samples. It therefore means that a compromise between defect removal and roughness has to be done since roughness tends to increase for high MRF removals.

4 MRF Polished Fused Silica Interface, Application to UV Optics

We analyzed the composition of the MRF polished interface on different samples as detailed in Table 1 using the protocol described in Sec. 2.4. Our aim was to evaluate the effect material removal and MRF process parameters on contaminants of the polished interface. Uniform removals (no figure correction) were performed on polished samples (no scratching performed).

Table 1 Magnetorheological finishing condition and volumetric removal rates (VRRs) for samples devoted to ICP analysis. All parts processed with Q22-XE, C10+, 50 mm wheel—ribbon height = 1.5 mm, wheel speed = 607 rpm, mixer speed = 100 rpm.

S/N	VRR (mm^3/ min)	Penetration depth (mm)	Delivery pump speed (rpm)	Material removal (μm)
11-0537 A	0.014	0.4	80	1
11-0537 B	0.026	0.45	80	1
11-0538 A	0.019	0.4	90	3
11-0539 A	0.026	0.5	95	5
11-0539 B	0.026	0.45	80	5

We first focus on iron pollution since MRF polishing fluid has carbonyl iron particles as magnetic particles. Figure 6 presents the evolution of Fe content in the interface of samples 11-0537 A and 11-0537 B. Both samples were polished to remove 1 μm using MRF parameters leading to a high VRR (11-0537 B) and a low VRR (11-0537 A). A power law fit of data from sample 11-0537 B is also added to this figure, data were insufficient to compute an equivalent fit for sample 11-0537 A.

It can be seen that iron penetration depth is independent from MRF conditions and that about 4 to 5 μm are polluted with iron coming from the MRF slurry. When removal is increased iron tends to go slightly deeper into the glass interface as depicted in Fig. 7. The iron-contaminated region is about 7 μm, rather constant when going from 3 to 5 μm of MRF removals.

Similar measurements were performed for cerium. Figure 8 shows that cerium pollution is independent of the material removal carried out and that cerium goes deeply into the substrates down to 7 μm.

These results demonstrate that the MRF slurry pollutes a depth of 5 to 7 μm from the top surface. Such a thickness can be considered as rather high, but it is indeed very similar to what is measured for a conventionally polished substrate. In a previous work, we investigated process-induced contamination on conventionally polished fused silica samples. We reported that fused silica samples polished with zirconium slurry had zirconium embedded in the interface down to 5 μm.[14]

We also damage-tested an MRF-polished part to evaluate the effect of this polishing layer on damage threshold at 351 nm. Two fused silica polished samples were prepared using a high-damage-threshold polishing process.[15] One side of one sample was polished on the MRF machine to remove 2 μm. Both samples were then damage-tested using the protocol detailed in Sec. 2.5. Damage threshold of the non-MRF-processed reference sample is 17 J/cm^2, (wavelength of 355 nm, pulse duration of 2.5 ns). The damage threshold of the MRF-processed sample is degraded with two types of damage morphologies as presented in Fig. 9. Images are obtained using the WLI described in Sec. 2.3 equipped with a 100× objective. At low fluences of 5 to 7 J/cm^2, a high density of micrometer-scale shallow pits is observed [see Fig. 9(a)]. These pits are often called "gray haze" and were attributed to the existence of heavy contamination of cerium in the glass interface.[26] This interpretation is in good concordance with ICP-AES

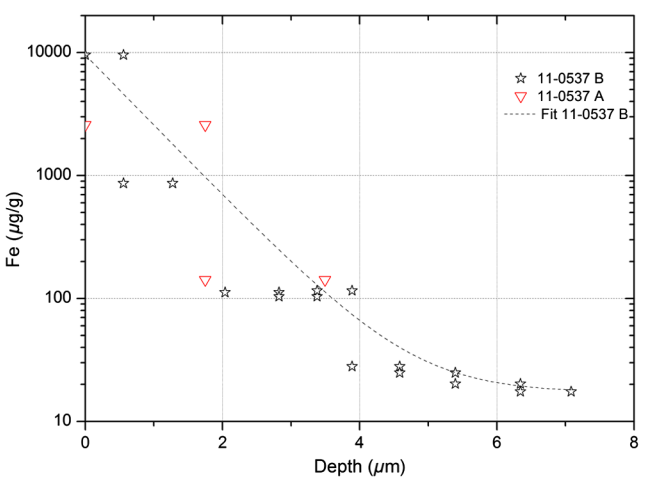

Fig. 6 Fe contamination measured on part 11-0537 A and 11-0537 B. Material removal of 1 μm in both cases. Power law fit of 11-0537 B presented in dash line.

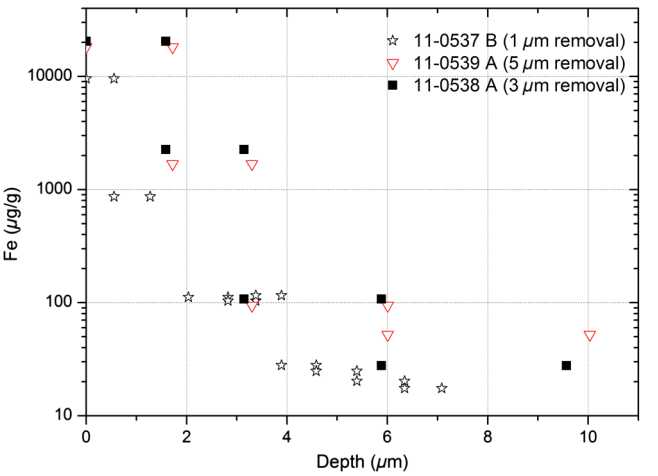

Fig. 7 Impact of MRF removal on iron contamination for different material removals.

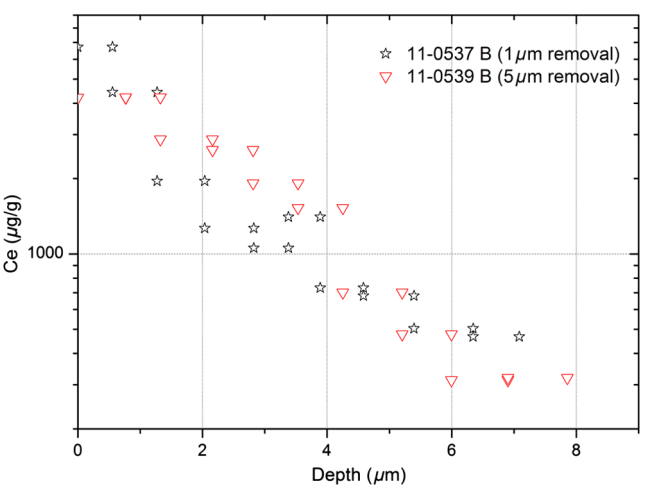

Fig. 8 Impact of MRF removal on cerium contamination.

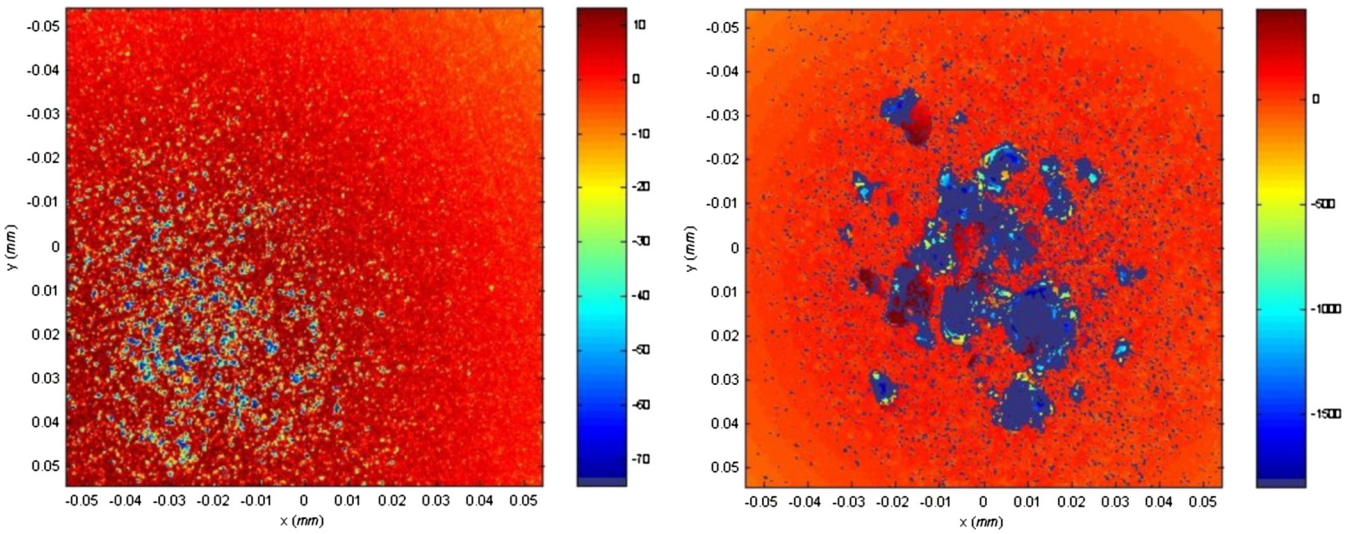

Fig. 9 Laser damage morphology of an MRF-processed silica part by WLI using a 100× objective. Depth scale expressed in nanometers. High-density pits are seen at low fluence (a), a larger damage is superimposed at high fluence (b).

measurements (Fig. 8) showing the existence of cerium in the glass interface. At higher fluence [Fig. 9(b)] damage evolves in a large damage typical of what is usually observed on fused silica polished parts, superimposed to the gray haze seen at lower fluences.

MRF polished surface consequently needs a wet etching to remove the polluted fused silica interface in order to achieve high damage threshold. This approach was retained with success by various authors.[27,28]

5 Summary

MRF can remove surface and subsurface defects existing on the fused silica polished surfaces. No MRF related defects were seen during our experiments apart from sleeks surrounding pre-existing scratches or digs. The VRR used during MRF processing seems to have a weak impact on the ability of the process to remove these defects. We also carried out ICP measurements to quantify composition and depth of the MRF-induced interface pollution; this interface includes both Beilby layer and potential contaminants diffusing in SSD. Up to 5 to 7 μm are polluted with MRF slurry elements such as iron and cerium (C10+ MRF slurry). MRF process parameters have weak impact on the characteristics of this interface (depth, composition). This depth is similar to what is seen for conventional polishing processes.

Acknowledgments

This work is supported by the Conseil Régional d'Aquitaine and is performed in the framework of the EFESO 2 project. R. Catrin was supported by a CEA/Marie Curie FP7 Eurotalents postdoctoral fellowship. The authors thank the Optical Metrology Lab from CEA for roughness and laser damage measurements as well as access to various experimental measurement setups.

References

1. W. Kordonsky et al., "Magnetorheological polishing devices and methods," U.S. Patent 5,449,313 (1993).
2. W. Kordonski, D. Golini, and S. Hogan, "System for abrasive jet shaping and polishing of a surface using magnetorheological fluid," U.S. Patent 5,971,835 (1999).
3. W. Kordonski and S. Jacobs, "Magnetorheological finishing," *Int. J. Mod. Phys. B* **10**(23–24), 2837–2848 (1996).
4. QED Technology, New York, http://www.qedmrf.com.
5. C. Miao, J. C. Lambropoulos, and S. D. Jacobs, "Process parameter effects on material removal in magnetorheological finishing of borosilicate glass," *Appl. Opt.* **49**(10), 1951–1963 (2010).
6. D. Golini et al., "Magnetorheological finishing (MRF) in commercial precision optics manufacturing," *Proc. SPIE* **3782**, 80–91 (1999).
7. P. Dumas et al., "Complete sub-aperture pre-polishing & finishing solution to improve speed and determinism in asphere manufacture," *Proc. SPIE* **6671**, 667111 (2007).
8. W. Messner et al., "Manufacturing meter-scale aspheric optics," *Proc. SPIE* **6671**, 667106 (2007).
9. J. Menapace et al., "MRF applications: on the road to making large-aperture ultraviolet laser resistant continuous phase plates for high-power lasers," *Proc. SPIE* **6403**, 64030N (2006).
10. F. Shi et al., "Magnetorheological elastic super-smooth finishing for high-efficiency manufacturing of ultraviolet laser resistant optics," *Opt. Eng.* **52**(7), 075104 (2013).
11. M. D. Feit and A. M. Rubenchik, "Influence of subsurface cracks on laser induced surface damage," *Proc. SPIE* **5273**, 264–272 (2004).
12. F. Y. Génin et al., "Role of light intensification by cracks in optical breakdown on surfaces," *J. Opt. Soc. Am. A* **18**(10), 2607–2616 (2001).
13. D. W. Camp et al., "Subsurface damage and polishing compound affect the 355 nm laser damage threshold of fused silica surfaces," *Proc. SPIE* **3244**, 356–364 (1998).
14. J. Neauport et al., "Polishing-induced contamination of fused silica optics and laser induced damage density at 351 nm," *Opt. Exp.* **13**(25), 10163–10171 (2005).
15. J. Neauport et al., "Concerning the impact of polishing induced contamination of fused silica optics on the laser-induced damage density at 351 nm," *Opt. Commun.* **281**(14), 3802–3805 (2008).
16. M. Schinhaerl et al., "Forces acting between polishing tool and workpiece surface in magnetorheological finishing," *Proc. SPIE* **7060**, 706006 (2008).
17. J. Seok et al., "Tribological properties of a magnetorheological (MR) fluid in a finishing process," *Tribol. Trans.* **52**(4), 460–469 (2009).
18. C. Miao et al., "Shear stress in magnetorheological finishing for glasses," *Appl. Opt.* **48**(13), 2585–2594 (2009).
19. M. Schinhaerl et al., "Comparison of different magnetorheological polishing fluids," *Proc. SPIE* **5965**, 596528 (2005).
20. R. Catrin et al., "Using STED and ELSM confocal microscopy for a better knowledge of fused silica polished glass interface," *Opt. Express* **21**(24), 29769–29779 (2013).
21. F. Rainer et al., "Development of practical damage mapping and inspection systems," *Proc. SPIE* **3492**, 556–563 (1999).
22. W. S. Rasband, "ImageJ," U. S. National Institutes of Health, Bethesda, Maryland, http://imagej.nih.gov/ij/ (1997–2014).

23. G. T. Beilby, "Surface flow in crystalline solids under mechanical disturbance," *Proc. R. Soc. London* **72**(477–486), 218–225 (1903).
24. T. Suratwala et al., "Sub-surface mechanical damage distributions during grinding of fused silica," *J. Non-Cryst. Solids* **352**(52–54), 5601–5617 (2006).
25. T. Suratwala et al., "Scratch forensics," *Opt. Photonics News* **09**, 12–15 (2008).
26. M. Kozlowski et al., "Depth profiling of polishing-induced contamination on fused silica surfaces," *Proc. SPIE* **3244**, 365–375 (1998).
27. J. Menapace et al., "Combined advanced finishing and UV-laser conditioning for producing UV-damage-resistant fused silica optics," *Proc. SPIE* **4679**, 56–68 (2002).
28. F. Shi et al., "Magnetorheological elastic super-smooth finishing for high efficiency manufacturing of ultraviolet laser resistant optic," *Opt. Eng.* **52**(7), 075104 (2013).

Biographies for the authors are not available.